1550/1310-nm Dual-Wavelength High-Power Laser Diode

Shintaro Morimoto, Hiroshi Mori, Atsushi Yamada, Yasuaki Nagashima, Motoaki Fujita, Shinichi Onuki, Hiroaki Yoshidaya, Kazuaki Mise

[Summary] We have developed a high-power, 1550/1310-nm, dual-wavelength laser diode for the optical time domain reflectometer. It has 1550 and 1310-nm active layers aligned in tandem. The 1550-nm light cavity consists of front and rear facets, while the cavity for the 1310-nm light consists of a front facet and a diffraction grating in the center of the chip. Output powers exceeding 150 mW were obtained for both light wavelengths by adjusting the grating and cavity lengths. A fiber coupling efficiency of 80% was achieved by using a partially tapered waveguide structure.

1 Introduction

The recent spread of optical fiber networks is increasing the demand for an optical time domain reflectometer (OTDR) supporting optical spectrum analysis in both the 1550 and 1310-nm bands. This is usually achieved using semiconductor laser diodes (LD) as the light sources for each of the 1550 and 1310-nm bands with multiplexing after coupling each light source to the fiber[1)].

However, not only does this type of structure increase the number of optical parts, it also prevents reduction of the volume of the optical module and increases the complexity of the mechanism for adjusting the optical axes. Consequently, we have developed a 1550/1310-nm dual-wavelength LD consisting of two active layers in tandem for the 1550 and 1310-nm bands and supporting output of both wavelengths from one point. We predicted that this dual-wavelength LD oscillates at 1550 nm by reflecting the light between two facets, as well as at 1310 nm by reflecting light between one facet and a grating located at the center of the waveguide. The actual prototype succeeded in dual-wavelength lasing from one chip. This article reports the evaluation results when mounted in a cylindrical fiber-coupling module for use as an OTDR light source.

2 Basic Concept of Dual Wavelength LD

We designed the following type of LD structure supporting simultaneous output of light in both the 1550 and 1310-nm bands[2)]. The 1550-nm light is not absorbed when it passes the 1310-nm active layer, but the 1310-nm light is absorbed when passing the 1550-nm active layer. Consequently, we arranged the reflective structures to select the wavelengths by placing the 1310-nm active layer at the output side with a diffraction grating at the boundary of both active layers preventing insertion of the 1310-nm band light into the 1550-nm band active layer (figure 1).

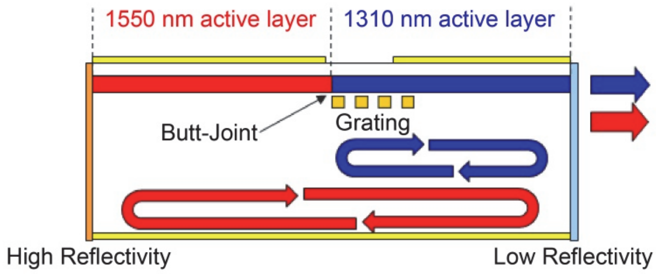

Figure 1 Principle of Dual-Wavelength Lasing

Using this type of configuration, the longer-wavelength 1550-nm band cavity is formed by reflections between the two end facets, and the 1310-nm band cavity is formed by reflections between the front facet and the diffraction grating in the center of the waveguide to output light of both wavelengths simultaneously. In other words, a dual-wavelength LD with single lens can be fabricated with a very simple structure for coupling to one single mode fiber (SMF).

3 Fabricated Device Structure

Figure 2 shows the structure of the 1550/1310-nm band dual-wavelength integrated LD. The 1550-nm band active layer consists of four quantum well layers of +1% compressively-strained InGaAsP and lattice-matched InGaAsP barrier layers. The Separated Confinement Heterostructure (SCH) layer has a graded index structure. On the other hand, the 1310-nm band active layer is a lattice-matched InGaAsP bulk layer.

The fabrication process is as follows. First, a diffraction grating with a pitch for a reflection wavelength of 1310 nm was formed on n-type InP substrate (design diffraction grating coupling coefficient κ = 163 cm^{-1}). The 1550-nm band active layer was grown on this layer. Next, the 1550 and 1310-nm active layers were butt-jointed by etching and regrowth. The butt-jointed 1550/1310-nm active layers were Mesa-stripe processed by etching. Next, the side of the mesa stripe was buried in the current block layer. Then, a p-InP cladding layer and a p-InGaAs contact layer were grown over the mesa stripe and current block layer. Next, each n and p electrode was deposited and then the end facets formed by cleavage were coated with a 95% high-reflectivity (HR) coating film on the 1550-nm side and a 6% low-reflectivity (LR) coating film on the 1310-nm side. Metal Organic Vapor Phase Epitaxy (MOVPE) was used for all growth processes and an isolation groove was introduced for electrical isolation between the 1550 and 1310-nm band regions.

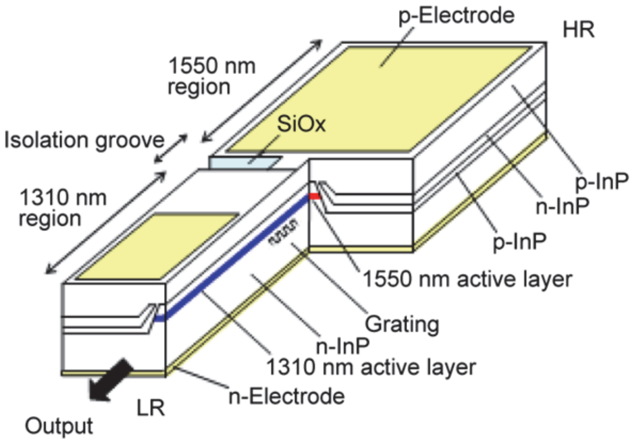

Figure 2 Schematic Structure of Device

4 Device Characteristics

4.1 L-I Characteristics

The 1550 and 1310-nm region lengths are fixed at 1 and 0.8 mm, respectively. The change in threshold current Ith and pulse output Po (1A) at diffraction grating region lengths from 0 to 200 µm is shown in figure 3. Without a diffraction grating, the diffraction grating region length is 0. In the 1310-nm band, the optical output is low when the threshold current is high. However, the optical output increases as the threshold current decreases as the grating region length increases. Conversely, for the 1550-nm band, it is clear that the characteristics are almost stable whether or not there is a diffraction grating. Consequently, the fabricated diffraction grating is confirmed as having good reflection characteristics for the 1310-nm band light. On the other hand, it is clear that it causes practically no loss in the 1550-nm band light. Moreover, measurements when changing the lengths for both the 1550 and 1310-nm band regions show the same tendency, although the absolute values are different.

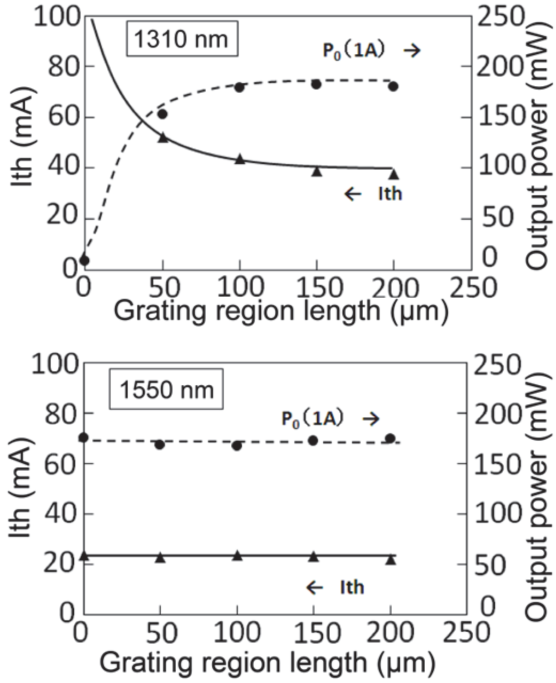

Figure 3 Dependence of Threshold Current and Optical Output on Grating Region Length

In addition, figure 4 shows the L-I characteristics when the diffraction grating region length is fixed at 150 µm and the 1550-nm band region length is fixed at 1.0 mm and the 1310-nm band region length (L_{1310}) is varied from 0.6 to 1.0 mm. The 1310-nm band characteristics clearly show improved output and saturation characteristics as the region length increases. Conversely, the L-I for the 1550-nm band show a reverse trend to the 1310-nm band characteristics, clarifying that the output for the passed 1550-nm band decreases as the 1310-nm band region length increases. This suggests that loss is caused when the 1550-nm band light passes through the 1310-nm band region and we suppose that this is mainly due to absorption in the sub-bands in the p-type cladding. Experiments using a fabrication with the 1310-nm band region fixed to 0.8 mm showed that the optical output power was almost equal for both wavelengths at 1A.

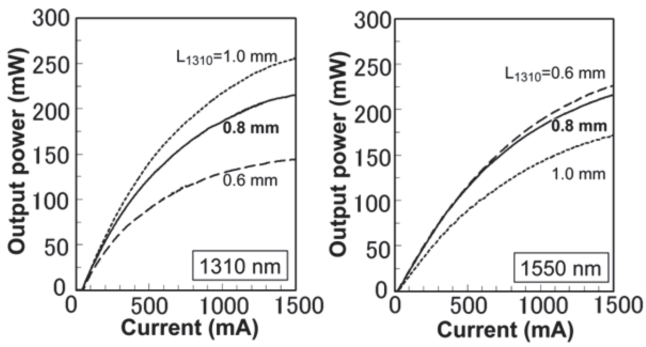

Figure 4 L-I Characteristics

4.2 Spectrum Characteristics

We observed the spectrum characteristics of the fabricated device. Figure 5 shows the spectrum for each lasing condition when injecting a 1-A pulse current into each region. The spectrum in the 1310-nm band has a comparatively narrow FWHM due to reflection from the grating, whereas in the 1550-nm band, the spectrum has a comparatively wide half width as a result of Fabry-Perot (FP) lasing. In addition, detailed observation of the 1550-nm band spectrum longitudinal mode spacing shows no effect of the diffraction grating and confirmed that lasing at both end facets is dominant.

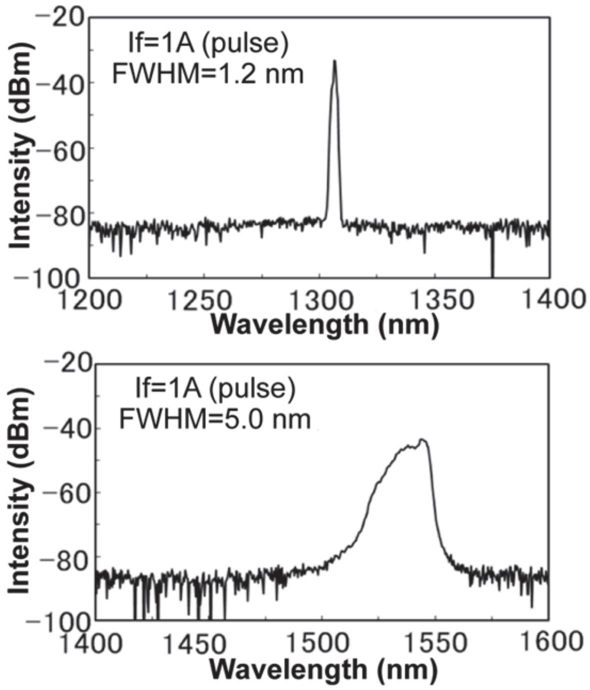

Figure 5 Lasing Spectra

Moreover, simultaneous lasing was confirmed by injecting current simultaneously to the 1550 and 1310-nm band regions while shorting the upper electrodes.

4.3 Far Field Pattern and Coupling Efficiency

First, we investigated the fiber coupling efficiency of a device fabricated with the same widths for the 1550-nm and 1310-nm band active layers. We measured the fiber coupling efficiency with an aspherical lens and SMF. A maximum coupling efficiency of 78% was obtained for the 1310-nm band. On the other hand, a maximum coupling efficiency of 50% was obtained for the 1550-nm band. Moreover, the image magnification obtained at the maximum coupling efficiency for both wavelengths was almost the same at 3.8x.

Far Field Pattern (FFP) measurements for the 1550-nm band showed that the shape in the horizontal direction was bimodal and clarified that interference was superimposed on the entire horizontal direction.

Consequently, we suppose that the low coupling efficiency with SMF in the 1550-nm band light is due to a higher-order horizontal mode occurring at passage through the 1310-nm band region as well as to an emission mode occurring at the butt-joint boundary. When considering OTDR applications, it is better if the fiber output is as high as possible to couple the fiber output directly to the OTDR dynamic range. As a result, two important themes are achieving high chip output for the 1550-nm band light as well as achieving high efficiency coupling with SMF.

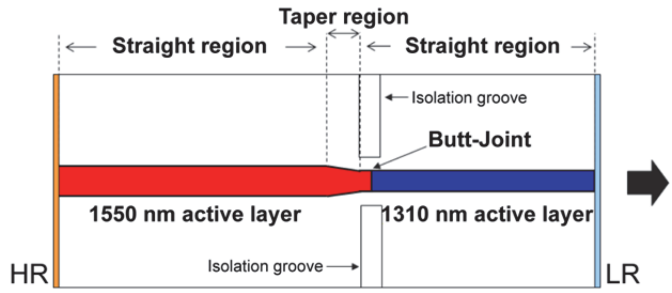

Figure 6 Tapered Waveguide Structure

As a result, based on the uniform-width-structure of the previous waveguide, to examine using a waveguide with a tapered structure to link the two regions, we set the 1550-nm band active layer width to the maximum width for fundamental horizontal mode operation, and then set the width of the waveguide in the fundamental horizontal mode so that higher-order horizontal modes would not occur when the 1550-nm band light passed through the 1310-nm region (figure 6).

Figure 7 shows the FFP in the horizontal direction for 1550-nm band light. With the tapered structure, the waveform becomes a single peak and all superimposed interference is removed, suggesting that when 1550-nm light passes via the 1310-nm region, the wave is guided in the fundamental horizontal mode and emission modes before and after the butt-joint are reduced. Moreover, it is also confirmed that the 1550-nm chip output is broadly constant irrespective of whether the waveguide has a tapered structure or not; it was possible to operate in the fundamental horizontal mode with no decrease in the 1550-nm band chip output. In addition, measuring FFP in the vertical direction showed no change with or without the taper structure and the shape was confirmed to be almost constant.

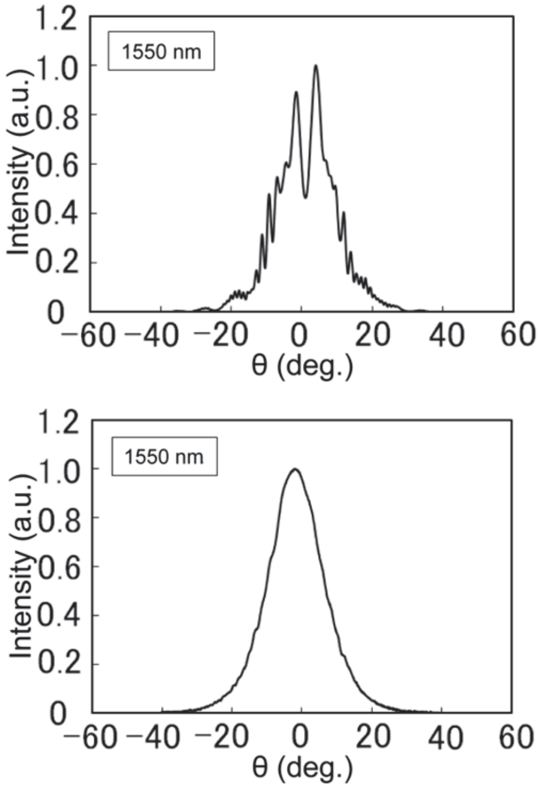

Figure 7 1550-nm Horizontal FFP
(Top: Without Taper; Bottom: With Taper)

On coupling a device with this tapered structure to an SMF using a lens, we obtained a coupling efficiency of about 80% for the 1550-nm band, which is a large improvement over the 50% coupling efficiency described previously without the tapered structure. Not only is the 80% coupling efficiency about equal to the 1310-nm band coupling efficiency, it is not inferior when compared with the coupling efficiencies of other discrete elements and SMF. Consequently, high-efficiency optical coupling can also be achieved using a tapered waveguide structure.

4.4 Reliability Test

A high-temperature aging test was performed at each wavelength under CW conditions. The test conditions used a constant drive current (ACC) to operate the LD at 70°C (figure 8). The median life at T_{LD} = 25°C with an activation energy of 0.4 eV estimated as a 20% decrease in optical output was 730,000 hours for the 1310-nm band and 1 million hours for the 1550-nm band, confirming that the device reliability is at a practical usage level.

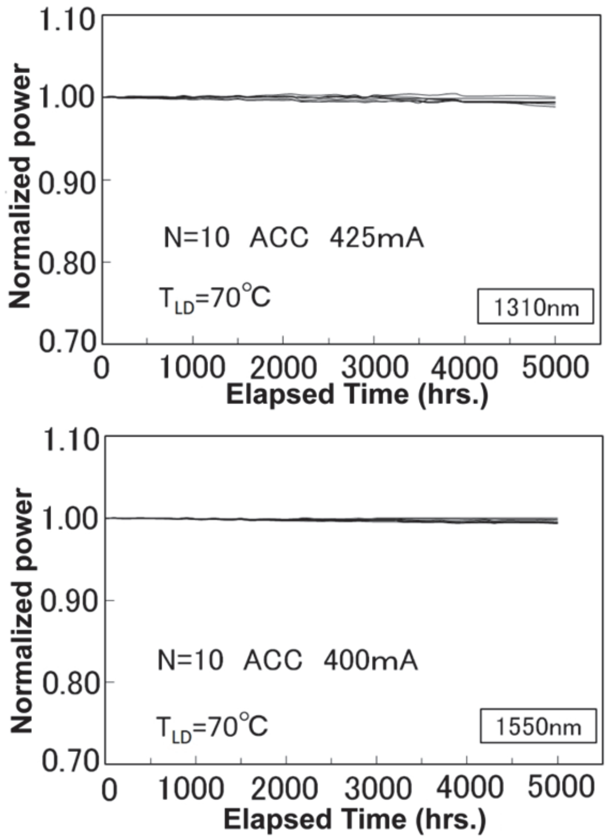

Figure 8 High-Temperature Aging Test

5 OTDR Applications

The following explains packaging of this device in a cylindrical module (figure 9) and introduces some results of evaluation of the module characteristics when installed in an OTDR.

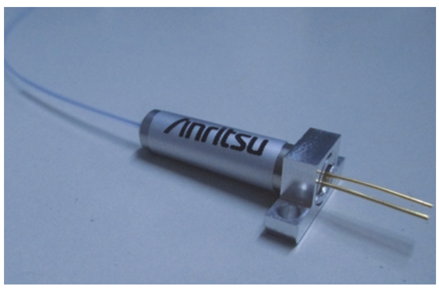

Figure 9 External View of Cylindrical Module

Figure 10 is the OTDR signal for a 1-µs pulse. The dynamic ranges for the 1550 and 1310-nm bands were 27.00 and 28.10 dB, respectively.

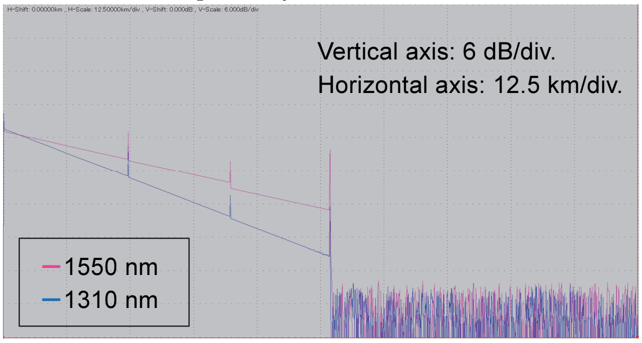

Figure 10 OTDR Signal

On the other hand, in an OTDR, the ripple characteristics caused by the light-source coherency are an important cause of degraded fiber loss measurement accuracy, etc.. The signal ripple is calculated as the difference between the measured power of the returned light and the value found by linear approximation using the least squares method. Figure 11 shows the signal ripple for each wavelength. Since this characteristic is determined by the spectrum width of the light source, there is a large difference for both wavelengths due to the difference in the spectral widths of both wavelengths shown in figure 5. Since the 1550-nm band light is generated between both end facets, it has the same spectrum width as a conventional FP-LD, resulting in about the same 0.02 dB of ripple when used in an OTDR. In contrast, the 1310-nm band light has a narrow spectrum width because it is reflected by the diffraction grating, and the larger ripple value of 0.06 dB is due to the higher optical interference. This is a point for future improvement.

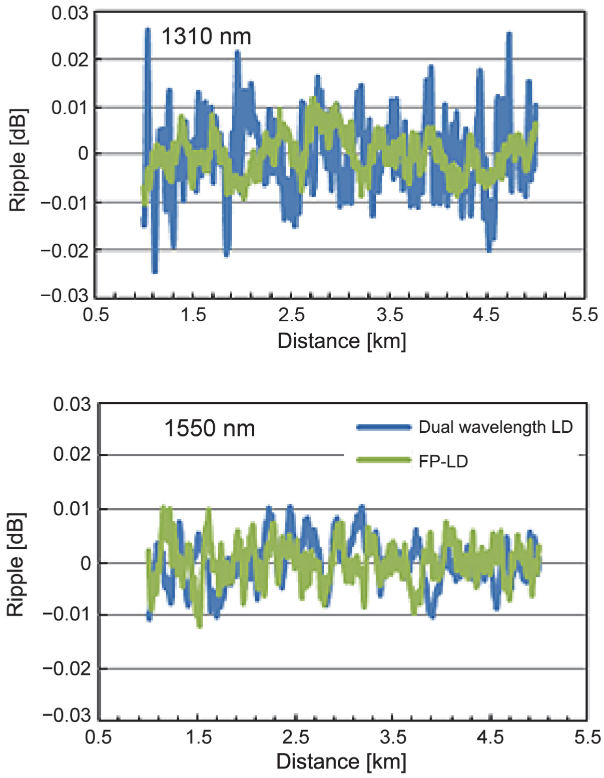

Figure 11 OTDR Signal Ripple Characteristics

6 Summary

We have developed and tested a dual-wavelength 1550/1310-nm LD outputting both wavelengths from a single exit point by fabricating two optically coupled active layers in tandem for the 1550 and 1310-nm bands with the 1550-nm light reflected by the front and rear facets, and the 1310-nm light reflected by one facet and a diffraction grating inserted in the center of the waveguide. The test results confirm the lasing for both wavelengths as well as high-output operation. In addition, we examined the 1550-nm band high output and the fundamental horizontal mode occurring across all regions. Using a tapered waveguide at the dual-wavelengths clarified the effectiveness in increasing the output power for the 1550-nm band and in maintenance of the fundamental horizontal mode. A 5000-h high-temperature aging test confirmed that the device had good reliability for practical use. Use as a light source was tested with an optical pulse tester, confirming satisfactory basic performance.

Future work on widening the spectrum width for the 1310-nm light is being investigated along with reducing the internal loss for the 1550-nm light.

References

1) "Development of Optical Time Domain ReflectometerMW9040B", ANRITSU TECHNICAL No.64 1992 (in Japanese)

2) "1550 nm/1310 nm Dual-Wavelength, High-Power Laser Diode", IEICE Society Conference 2012, C-4-12,2012 (in Japanese)

Authors

Shintaro Morimoto
Anritsu Corporation
Optical Device Development Dept.

Hiroshi Mori
Anritsu Corporation
Optical Device Development Dept.

Atsushi Yamada
ANRITSU DEVICES CO.,LTD.
Management Administration Dept.

Yasuaki Nagashima
Anritsu Corporation
Optical Device Development Dept.

Motoaki Fujita
ANRITSU INDUSTRIAL SOLUTIONS CO.,LTD.
Design Quality Assurance Dept.

Shinichi Onuki
Anritsu Corporation
Optical Device Development Dept.

Hiroaki Yoshidaya
Anritsu Corporation
Optical Device Development Dept.

Kazuaki Mise
Anritsu Corporation
Optical Device Development Dept.